Correction Procedure of Wave Signals for a Viscoelastic Split Hopkinson Pressure Bar

Jacek JANISZEWSKI[1*], Witold BUŻANTOWICZ[1],
Paweł BARANOWSKI[2]

[1]*Faculty of Mechatronics and Aerospace, Military University of Technology,*
[2]*Faculty of Mechanical Engineering, Military University of Technology,*
2 Sylwestra Kaliskiego St., 00-908 Warsaw, Poland
[*]*corresponding author, e-mail: jacek.janiszewski@wat.edu.pl*

Abstract. A polymeric split Hopkinson pressure bar technique (SHPB) is preferred for testing materials with low mechanical impedance. However, the use of polymeric bars requires additional analysis for data reduction, temperature complications and additional restrictions compared with traditional metallic pressure bars. A viscoelastic material, such as PMMA, exhibits both wave attenuation and wave dispersion. When a wave travels through a polymer bar, the wave amplitude decreases due to attenuation and the wave shape becomes distorted. Therefore, signals measured at given positions on a viscoelastic bar do not represent the pulse at another position along the pressure bar without complex corrections. This paper is concerned with the problem of correction of dispersion and attenuation of waves in the viscoelastic SHPB. It has been demonstrated that the Fast Fourier Transform (FFT) spectral analysis method used to reconstruct wave profiles on the measured signals which are being distorted by wave attenuation and dispersion effects is valid and allows for obtaining satisfactory results for tire rubber.
Keywords: solid mechanics, viscoelastic bar, split Hopkinson pressure bar

1. INTRODUCTION

The hybrid/multilayer armour systems are finding more and more increasing application in light-weight ships, vehicles, aircrafts and bulletproof vests [1-3]. In the past armour systems have been conventionally monolithic, typically composing of a high strength steel plate. Over the last few decades, however, there is an increasing demand for armour systems providing maximum ballistic protection at a minimum weight. Among the novel recent approaches, multilayer armour systems seem to be the most perspective [3]. These armour systems consist of a number of layers, which each serving a specific purpose. In general, hard layers (e.g. armour steel, ceramic) and layers made of low-impedance materials, in particular elastomers can be distinguished.

More recently, many types of elastomers (e.g. rubber, polyuera) have been applied as a blast/ballistic protection materials of combat vehicles [4, 5]. The specific properties of elastomers, such as: high toughness to density ratio, capability to accommodate large deformations and possession of high damping characteristics, make them suitable for employment in the dissipation of kinetic energy associated with impacts and shocks.

The stress-strain responses of elastomers generally exhibit nonlinear rate-dependent elastic behaviour and they are sensitive to loading conditions: the rate and the state of loading [2, 6]. Therefore, a number of significant problems can occur during an optimization of multilayer armour design, containing an elastomer layer or matrix, using the computer simulation. For this reason, experimental investigations of a mechanical response of elastomers over a wide range of strains and strain rates, in particular high-strain-rates, are essential.

The SHPB (Split Hopkinson Pressure Bar), also called the Kolsky bar, is a commonly used experimental technique to study mechanical properties of materials under dynamic loading at the strain rate of $10^3 \div 10^4$ s^{-1} [7]. The SHPB setup usually consists of striker bar and two long bars called incident bar and transmitted bar, with the same diameter and material (typically high strength material like maraging steel). During a test the striker is launched using highly compressed gas and impacts the incident bar. This generates the trapezoidal stress impulse (incident wave) which travels through the impacted bar.

When the elastic wave reaches the specimen, due to the mismatch of mechanical impedances between the bar and specimen material, part of the incident wave is reflected back (reflected wave) and the rest of the incident wave is transmitted through the specimen. It is compressed at high rates and rest of the wave travels to the transmission bar as a transmitted wave.

The incident and reflected signals are recorded by the strain gages, which are glued on the incident bar whereas the transmitted signals are sensed by the strain gages located on the transmission bar.

The above-described setup configuration with two long bars and the short specimen between them was introduced by Kolsky [8].

In general, the SHPB technique has been widely used to determine the dynamic properties of a variety of engineering materials, such as metals and theirs alloys, ceramics, composites and shape memory alloys [9]. A soft materials or generally speaking, low impedance materials, such as elastomers [10], foams [11] and even biological tissues [12] have been also tested by the use of the SHPB. However, if the specimen is a soft material, for example, rubber, application of the SHPB technique needs to solve many technical and methodological problems. These problems arise mainly because the transmitted signal may be too weak to be measured due to large mismatch of impedance between the specimen and the metallic bars. The specimen thickness also influences the attenuation of transmitted signal because the stress wave propagating in soft material has relatively low velocity [13]. Due to these limitations, many modifications of the conventional SHBP technique were developed.

The simplest approach is to increase the sensitivity of gauges recording transmitted pulse. For example, the authors of paper [13] used piezoelectric quartz gauges embedded on aluminium bars. The second method includes the reduction of mechanical impedance differences between the bars and specimen using mainly three options: (1) by modifying the cross section of the specimen, (2) by altering the cross section of the pressure bar (e.g. using a hollow transmission bar. [14]), and (3) by changing the material of the pressure bars, e.g. by replacing metals bars with polymeric bars [15]. The latter is very often chosen by many investigators.

The substitution of polymeric bars for metallic ones, however, causes many problems due to the viscoelastic nature of the polymer material [16, 17]. For metal/elastic bars, it is assumed that the wave signals, which are determined from strain measured by strain gages, are not only known at the measuring points but everywhere along the bar because the elastic wave can be shifted to any distance by knowing the wave propagation theory. Thus, the transmitted wave can be shifted to transmitted bar-specimen interface to calculate transmitted force and velocity, whereas incident force and velocity can be obtained from incident and reflected signals shifted to incident bar-specimen interface. Unfortunately, this procedure is not valid for polymeric bars because of the attenuation and dispersion of wave pulse during its propagation along the bar. Therefore, the correction of the wave signals is necessary for the use of a viscoelastic SHPB.

There are two approaches of the wave signals correction. The first method is based on theoretical viscoelastic constitutive equation and characteristics theory of wave propagation [18].

This approach, however, requires the knowledge of a rheological model and its constants, what is associated with additional efforts. An alternative approach is to use a spectral analysis for correction of wave pulses [15, 19, 20].

This study is focused on a spectral analysis and wave shifting procedure, which was applied to a PMMA split Hopkinson pressure bar setup developed at the Military University of Technology.

2. SPECTRAL ANALYSIS OF VISCOELASTIC WAVES

The wave dispersion and attenuation in the viscoelastic SHPB can be corrected by the use of a digital signal processing (DSP) methods. Especially, Fast Fourier Transform (FFT)-based spectral analysis algorithms are preferred for reconstruction or prediction of wave signal shape at the considered point [19, 20]. The correction procedure is composed of two major steps: (1) identification of the attenuation factor and wave number for each frequency component of the wave, and (2) restoration of the frequency spectrum of the wave to be corrected or predicted for the selected position on the bar (shifting procedure).

2.1. Identification procedure of the attenuation factor and wave number

Let assume that the strain gage positions are placed at a viscoelastic bar, and stress wave is generated by impact of a striker, as shown in Fig. 1. Then, the measured wave signals are $u_1(t)$ at x_1 and $u_2(t)$ at x_2.
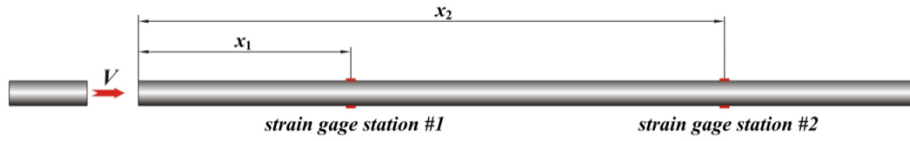
Fig. 1. Schematic diagram of strain gage stations placement

Using a proper time window and sampling rate allows us to achieve the digital form of wave signal from each strain gage position, $u_1[\tau]$ and $u_2[\tau]$, respectively, where τ is the sample number. Their corresponding spectrums, calculated *via* FFT, are as follows:

$$U_1[\omega] = \text{FFT}\{u_1[\tau]\} = \sum_n U_{1n} \, e^{i\phi_{1n}}$$
$$U_2[\omega] = \text{FFT}\{u_2[\tau]\} = \sum_n U_{2n} \, e^{i\phi_{2n}}$$

(1)

where U_{1n} and U_{2n} are the amplitudes, ϕ_{1n} and ϕ_{2n} are the phases of the spectral components.

The attenuation factor α_n and the wave number k_n (representing wave dispersion) for each frequency component can be estimated from digital representations of the measured wave signals at x_1 and x_2 using the following relations [20, 21]:

$$\hat{\alpha}_n = \frac{\ln U_{1n} - \ln U_{2n}}{x_2 - x_1} \tag{2}$$

and

$$\hat{k}_n = \frac{\phi_{1n} - \varphi_{2n}}{x_2 - x_1} \tag{3}$$

It should be noticed that theoretical and estimated values of attenuation factors and wave numbers are generally different, $\alpha_n \neq \hat{\alpha}_n$ and $k_n \neq \hat{k}_n$. However, since the condition of linearity is satisfied, that means:

$$x = l\left(x_2 - x_1\right) \tag{4}$$

where x is the position of the wave to be corrected or predicted, and l is the integer, then the estimated values can be used for the purposes of the restoration: attenuated and dispersed waves are corrected precisely, even if the estimated values are different from their real ones.

2.2. Wave signal shifting procedure

The wave $u_c(t)$ at the position of x_c needs to be corrected, and the wave $u_p(t)$ at the position of x_p needs to be predicted based on the measured wave $u_m(t)$ at the position of x_m, as shown in Fig. 2.
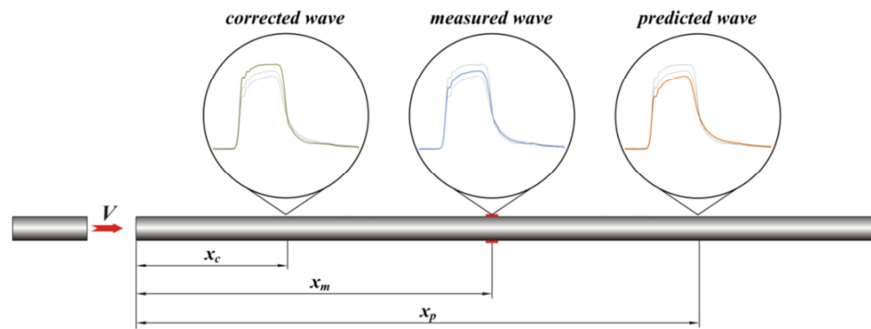
Fig. 2. The corrected, measured and predicted waves

According to the theory of spectral analysis of wave motion [21], for one-dimensional linear viscoelastic wave propagation, a bar transfer function can be expressed as:

$$G[\omega] = \sum_n G_n = \sum_n e^{-(\alpha_n + i k_n)x} \tag{5}$$

where x is the position of the considered point.

Taking above into account, the frequency spectrum of the wave $u_c(t)$ is corrected using the following equation [20]:

$$U_c[\omega] = \sum_n U_{mn} G_n e^{i\phi_{mn}} = \sum_n U_{mn} e^{i\phi_{mn}} e^{-(\alpha_n + i k_n)\Delta x_c} \tag{6}$$

where

$$\Delta x_c = x_c - x_m \tag{7}$$

U_{mn} and ϕ_{mn} are the amplitude and phase components taken from the FFT of the wave signal $u_m(t)$ measured at the position of x_m respectively. Finally, the discrete representation $u_c[\tau]$ of the corrected wave signal $u_c(t)$ at x_c is calculated using the IFFT, as given below:

$$u_c[\tau] = \text{IFFT}\{U_c[\omega]\} \tag{8}$$

In the case of the predicted wave signal $u_p(t)$ the procedure is analogous.

3. WAVE SHIFTING PROCEDURE VALIDATION

3.1. Experimental setup

The spectral analysis of viscoelastic wave pulses was performed using the algorithm developed in a Matlab software environment. As an input data, the signals collected by a high-frequency data acquisition system applied in the viscoelastic SHPB setup (Fig. 3) were used. The setup consisted of a bar system, which included 1218 mm long incident and transmission bars and air pressure gun, which launched 300 mm long striker bar. Both the incident and transmission bars and the striker had a common diameter of 12.00 mm and were made of commercial PMMA (plexiglass). Each bar was supported by 4 linear bearing stands, which were mounted on the optical bench allowing for precise alignment of the bars system.

Fig. 3. The PMMA split Hopkinson pressure bar set-up

The viscoelastic strain signals in the incident and transmitted bars were captured using a pair of strain gages attached symmetrically on the opposite surfaces of the bars and in theirs middle length. The strain gages were connected to the opposite legs of the Wheatstone bridge, which was a half bridge configuration. In the other legs of the bridge the dummy resistors were mounted, which resistance matched the strain gages resistance. The typical electrical strain gages of 1.6 mm gage length were used (CEA-13-062UW-350, Vishay Micro Measurements). The amplified signals of the strain gages were recorded at a frequency of 1 MHz using the signal conditioning unit (SGA-0B V5 Wheatstone bridge with signal conditioning amplifiers, ESA Messtechnik) and the data acquisition system (LeCroy WJ354A high-speed digital oscilloscope). The raw signals from the strain gages conditioned with the applied measuring equipment are shown in Fig. 4a for one-bar configuration, and in Fig. 4b for the connected incident and transmission bars.

Fig. 4. The raw viscoelastic wave signals measured by the strain gages:
(a) incident and reflected signals for one-bar configuration;
(b) incident and transmitted signals for the connected incident and transmission bars

3.2. Results

As it can be seen from Figs. 4a and 4b, the viscoelastic nature of wave propagation in the PMMA bars is clearly evident by the attenuation (amplitude decreasing) and dispersion (shape changing) of signals. The validation of the wave shifting procedure was carried out for the test presented in Fig. 4b. For this experiment, strain gages were attached on the bars in the position as it is presented in Fig. 5.
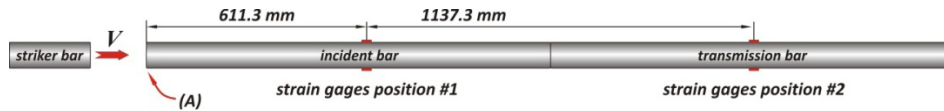
Fig. 5. Schematic diagram of real strain gages placement on the bars

Spectral analysis of viscoelastic waves began from calculation of the attenuation coefficient $\alpha(\omega)$ and the phase velocity $C(\omega)$ accordingly to papers [19, 20]. Fig. 6a shows that the attenuation coefficient changes become significant at the frequencies exceeding 3 kHz. However, the attenuation coefficient reaches a plateau for frequencies range between 10 and 17 kHz, and it increases further with larger frequency. For approximately 25 kHz the attenuation coefficient decreases rapidly with increasing frequency to ~30 kHz. The changes of the phase velocity are also substantial (Fig. 6b). It increases initially to reach maximum at 2 kHz, and next decreases with increasing frequency. Similarly to the attenuation coefficient, the phase velocity curve has plateau at a frequency range of between ~11 and ~20 kHz. The nature of changes of the attenuation coefficient and the phase velocity for the PMMA bar presented in Fig. 6 are coincident with the data presented in [22, 23].
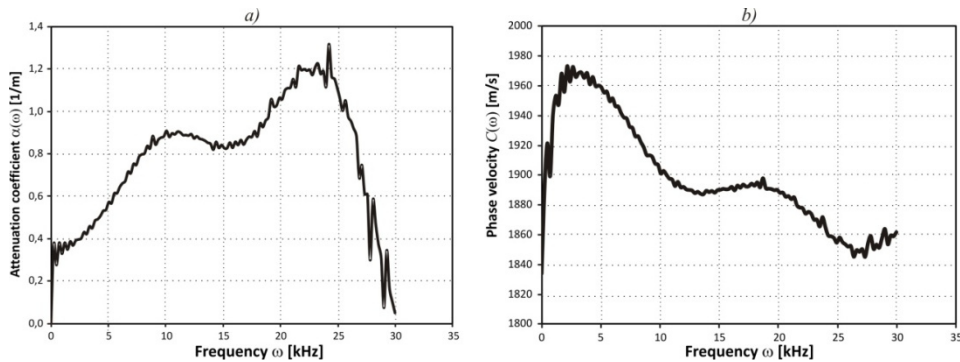
Fig. 6. Attenuation (a) and phase velocity (b) for the PMMA bars

On the basis of spectral analysis results, the waves shifting procedure was performed for the selected positions on the bar. The positions of wave shifting were so chosen in order to compare the reconstructed signal to the measured one. Figure 7 shows corrected, predicted and measured wave profiles at the points denoted *A*, #1 and #2, respectively (see Fig. 5). Figure 7a presents the corrected signals for the position *A*, which were reconstructed on the basis of the measured incident and transmitted signals. Similarly, the comparison of reconstructed and measured signals was made for positions #1 (Fig. 7b) and #2 (Fig. 7c). From the presented data in Fig. 7, the excellent correspondence between the corrected and predicted wave profiles (red line) and measured signals (black line) can be noticed. Therefore, authors assume that the procedure of the wave shifting was made properly.

The validity of the test apparatus and the method used to correct for wave attenuation and dispersion effects was also assessed by comparing the stress-strain relations for rubber specimens, which were tested using two different SHPB setup configurations i.e.: one equipped with the PMMA bars and the second with Al 7075-T6 bars. The dimensions of the applied Al 7075-T6 bars and data acquisition system were the same as in the case of the PMMA bars (see section 3.1). However, this time the PMMA bars were equipped with three sets of strain gages, i.e.: two strain gages sets were attached on the incident bar (47.1 mm and 565.3 mm far from impact surface), whereas one set of strain gages was glued in the middle of a transmission bar. The tire rubber was chosen as a tested material. Dimensions of specimens were as follows: diameter – 6 mm; thickness – 1.2 and 2 mm for the Al 7075-T6 and the PMMA bar configurations respectively.

On the basis of signals, obtained from strain gages attached on incident bar the spectral analysis and wave shifting procedure were performed for reflected and transmitted signals. For the Al 7075-T6 SHPB configuration, the standard elastic analysis of experimental data was applied (dumping and dispersion effects are insignificant) [7, 24].
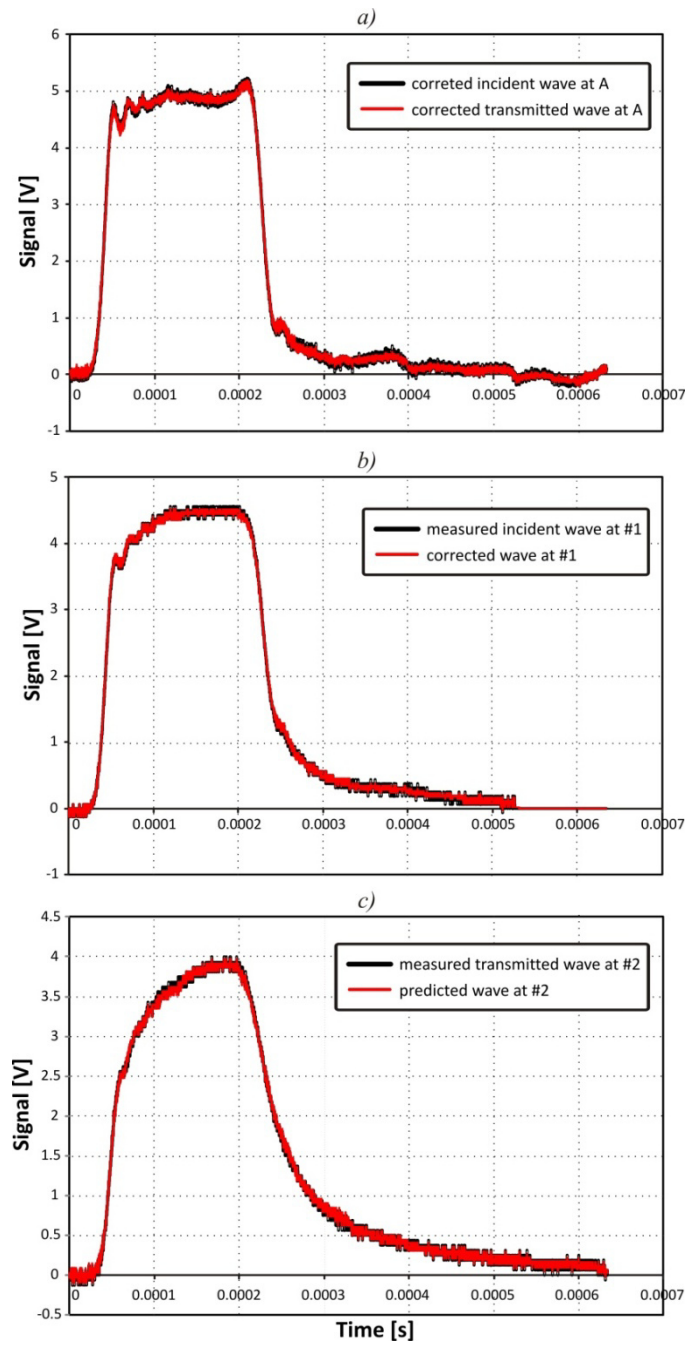
Fig. 7. Comparison of corrected, predicted, and measured wave profiles
for the position points A, #1 and #2

In Fig. 8, there were presented stress histories, which were calculated on the basis of measured and reconstructed wave signals.
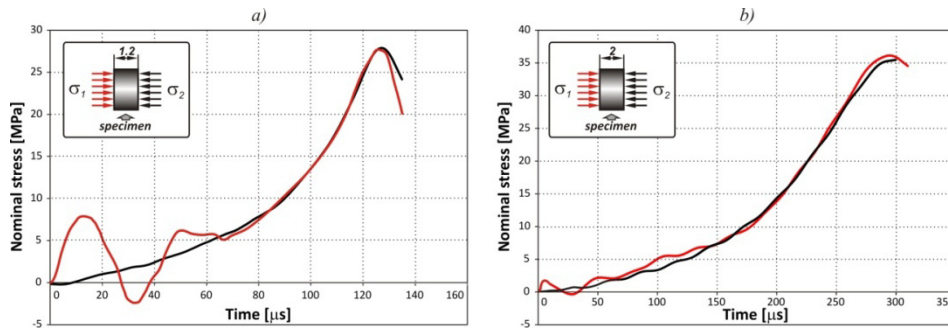
Fig. 8. Comparison of stresses at the front σ_1 and the rear σ_2 ends of rubber specimens tested with the use of the Al 7075-T6 bars (a) and the PMMA bars (b)

Stress curves in Fig. 8 represent stress conditions on the front σ_1 (red line) and the rear σ_2 (black line) ends of specimens. In each case, the impact velocity of striker bars was comparable and it was about 6 m/s. However, the stress equilibrium state was different for each experiment. The specimen tested with aluminum alloy SHPB deformed initially non-uniformly, and only after 60 microseconds stress equilibrium was achieved. In the case of the experiment with PMMA bars, non-equilibrium of stresses was also observed on specimen interfaces during initial stage of deformation, but non-equilibrium degree was significantly lower. First of all, it is the result of differences at rates of strain. Despite similar impact velocity, strain rate during experiment with aluminium alloy bars was higher ($\dot{\varepsilon} \approx 5700$ s^{-1}), because specimen length was shorter than the one during PMMA bar experiment. Moreover, rise times of incident wave for both experiments were very different from each other: 12 µs vs. 76 µs for the aluminium alloy and the PMMA bars, respectively.

The long rise time for PMMA bars is, on the one hand, the result of wave dissipation, but on the other hand, due to the application of the wave shaper (small disc with 4 mm diameter and 0.3 mm thickness made of polyethylene sheet). It should also be noted here that a loading duration of specimen during the PMMA bar experiment was considerably long (approx. 290 µs), whereas in the second case it was only 126 µs. It is due to lower propagation velocity of viscoelastic wave in the PMMA bar ($C_o \approx 1800$ m/s) in comparison to wave velocity in aluminium alloy bar ($C_o = 5117$ m/s). All aforementioned observations are consistent with predictions and thus they prove the validity of the method used to correct the wave attenuation and dispersion effects.

The correctness of the wave shifting procedure was also confirmed by the selected results collected in Fig. 9, where nominal stress-strain curves obtained from the experiments with the Al 7075-T6 and the PMMA bars were compared.

It is commonly known that rubber and other elastomers are very sensitive to the rate of strain [9, 24].

Hence, for the Al 7075-T6 SHPB experiment which was perform with high strain rate of 5700 s^{-1}, stress-strain relations (red curve) lies higher for strains above 0.3 than stress-strain curve (black) calculated from the PMMA SHPB experiment for which strain rate achieved lower value of 3800 s^{-1}.
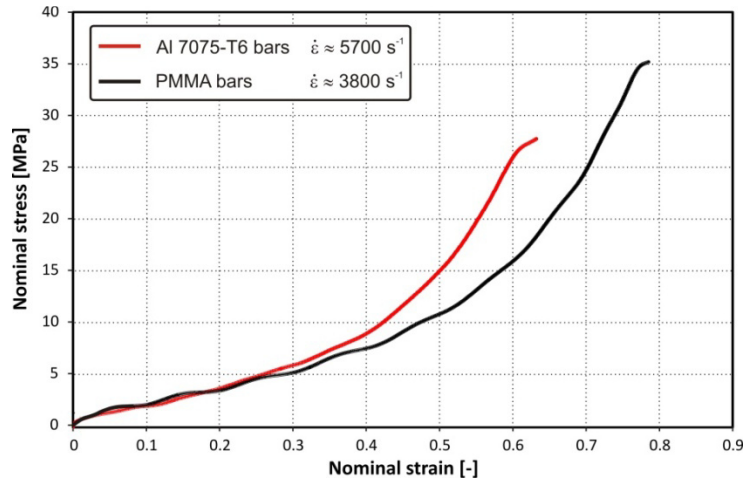
Fig. 9. Nominal stress-strain curves of tire rubber in various test conditions

4. SUMMARY REMARKS

The SHPB testing of soft materials with the use of the polymeric bars gives several benefits, such as e.g. increase in sensitivity of experimental setup and reduction of mechanical impedance mismatch. However, the use of polymeric SHPB technique requires additional analysis for data reduction, temperature complications, and additional restrictions compared with traditional metallic pressure bars. This is mainly caused by distorted wave propagation, i.e. exhibition of significant stress-wave attenuation and wave dispersion due to time and frequency dependency.

This paper is focused mainly on the problem of correction of the dispersion and attenuation of waves in the viscoelastic SHPB. A wave shifting procedure is presented in order to apply in the PMMA split Hopkinson pressure bar experiments. It has been demonstrated that the Fast Fourier Transform spectral analysis method used to reconstruct wave profiles on the measured signals being distorted by wave attenuation and dispersion effects is valid and allows us to obtain satisfactory results for low-impedance materials such as the tire rubber presented in the paper.

REFERENCES

[1]   Grujicic M., B. Pandurangan, B. D'entremont, 2012. „The role of adhesive in the ballistic/structural performance of ceramic/polymer–matrix composite hybrid armor". *Materials and Design* 41 : 380-393.

[2]   Grujicic M., B. Pandurangana, T. Hea, B.A. Cheesemanb, C.F.Yenb, C.L. Randow. 2010. „Computational investigation of impact energy absorption capability of polyuria coatings via deformation-induced glass transition". *Materials Science and Engineering* A 527 : 7741-7751.

[3]   Nilakantan Gaurav, Steven Nutt. 2014. „Effects of clamping design on the ballistic impact response of soft body armor". *Composite Structures* 108 :137-150.

[4]   Roland C.M., D. Fragiadakis, R.M. Gamache. 2010. „Elastomer–steel laminate armor". *Composite Structures* 92 : 1059-1064.

[5]   Ackland Kathryn, Christopher Anderson, Tuan Duc Ngo. 2013. „Deformation of polyurea-coated steel plates under localised blast loading". *International Journal of Impact Engineering* 51 : 13-22.

[6]   Pouriayevali Habib, Y.B. Guo, V.P.W. Shim. 2012. „A constitutive description of elastomer behaviour at high strain rates – A strain-dependent relaxation time approach". *International Journal of Impact Engineering* 47 : 71-78.

[7]   Chen Weinong, Bo Song. 2011. *Split Hopkinson (Kolsky) Bar, Design, Testing and Applications*, Springer.

[8]   Kolsky Herbert. 1949. „An investigation of the mechanical properties of materials at very high strain rates of loading". *Proc. Phys. Soc.*, B62 : 676-700.

[9]   Gray III George Rusty. 2000. ASM Handbook: Mechanical Testing and Evaluation,. In *Materials Park*: (ed. Kuhn H., D. Medlin D.), 939-1270. ASM International.

[10]   Shima Jongmin, Dirk Mohr. 2009. „Using split Hopkinson pressure bars to perform large strain compression tests on polyurea at low, intermediate and high strain rates". *International Journal of Impact Engineering* 36 : 1116-1127.

[11]   Liua Jiagui, Dominique Saletti, Stéphane Pattofattoc, Han Zhaoa. 2014. „Impact testing of polymeric foam using Hopkinson bars and digital image analysis". *Polymer Testing* 36 : 101-109.

[12]   Trexler M.M., A.M. Lennon, A.C. Wickwire, T.P. Harrigan, Q.T. Luong, J.L. Graham, A.J. Maisano, J.C. Roberts, A.C. Merkle. 2011. „Verification and implementation of a modified split Hopkinson pressure bar technique for characterizing biological tissue and soft biosimulant materials under dynamic shear loading". *Journal of the Mechanical Behavior of Biomedical Materials* 4(8) : 1920-1928.

[13] Chen Weinong, F. Lu, B. Zhou. 2000. „A Quartz-crystal-embedded Split Hopkinson Pressure Bar for Soft Materials". *Exp. Mech.* 40 (1) : 1-6.

[14] Chen Weinong, B. Zhang, M.J. Forrestal. 1999. „A split Hopkinson bar technique for low-impedance materials". *Exp. Mech.* 39 (2) : 81-85.

[15] Zhao Han, Gérard Gary, Janusz Roman Klepaczko. 1997. „On the use of a viscoelastic split Hopkinson pressure bar" *International Journal of Impact Engineering* 19 (4) : 319-330.

[16] Casem Daniel T., William L. Fourney, Peter Chang. 2003. „A Polymeric Split Hopkinson Pressure Bar Instrumented with Velocity Gages". *Experimental Mechanics* 43 (4) : 420-427.

[17] Chen Weinong, B. Zhang, M.J. Forrestal. 1999. „A Split Hopkinson Bar Technique for Low-impedance Materials" *Experimental Mechanics* 39 (2) : 81-85.

[18] Wang Lili, K. Labibes, Z. Azari, G. Pluvinage. 1994. „Generalization of Split Hopkinson Bar Technique to Use Viscoelastic Bars". *Int. J. Impact Eng.* 15 : 669-686.

[19] Bacon C. 1998. „An experimental method for considering dispersion and attenuation in a viscoelastic Hopkinson bar". *Experimental Mechanics* 38 (4) : 242-249.

[20] Cheng Z.Q., J.R. Crandall, W.D. Pilkey. 1998. „Wave dispersion ant attenuation in viscoelastic split Hopkinson pressure bar". *Shock and Vibration* 5 : 307-315.

[21] Doyle James F. 1989. *Wave Propagation in Structures – An FFT-Based Spectral Analysis Methodology*. New York: Springer-Verlag.

[22] Zhao Han, Gérard Gary. 1995. „A three dimensional analytical solution of the longitudinal wave propagation in an infinite linear viscoelastic cylindrical bar. Application to experimental techniques". *J. Mech. Phys. Solids* vol. 43 (8) : 1335-1348.

[23] Sana Hafiz, Ullah Butt, Pu Xue. 2014. „Determination of the wave propagation coefficient of viscoelastic SHPB: Significance for characterization of cellular materials". *International Journal of Impact Engineering* 74 : 83-91.

[24] Song Bo, Weinong Chen. 2003. „One-dimensional dynamic compressive behaviour of EPDM rubber". *Journal of Engineering Materials and Technology* 125 : 294-301.